Defective targeting of hemojuvelin to plasma membrane is a common pathogenetic mechanism in juvenile hemochromatosis

Laura Silvestri,[1] Alessia Pagani,[2] Claudia Fazi,[2] Gianmario Gerardi,[3] Sonia Levi,[1,2] Paolo Arosio,[3] and Clara Camaschella[1,2]

[1]San Raffaele Scientific Institute, Dibit, Milan, Italy; [2]University Vita-Salute San Raffaele, Milan, Italy; [3]Dipartimento Materno Infantile e Tecnologie Biomediche University of Brescia, Italy

Hemojuvelin (HJV) positively modulates the iron regulator hepcidin, and its mutations are the major cause of juvenile hemochromatosis (JH), a recessive disease leading to iron overload. Defective HJV reduces hepcidin up-regulation both in humans and in *Hjv*-deficient mice. To investigate the JH pathogenesis and the functional properties of human HJV we studied the biosynthesis and maturation of 6 *HJV* pathogenic mutants in HeLa and HepG2 cells. We show that proteolytic processing is defective in mutants F170S, W191C, and G320V, but not in G99V and C119F. Moreover, we show that mutants G99V and C119F are targeted to the cell surface, while F170S, W191C, G320V, and R326X (lacking the glycosilphosphatidylinositol [GPI] anchor) are mainly retained in the endoplasmic reticulum, although all mutants are released as soluble forms (s-HJV) in a proportion that is modulated by iron supplementation. Membrane HJV (m-HJV) is mainly composed of the cleaved protein, and its level is increased by iron in wild-type (WT) mice but not in the mutants. Altogether, the data demonstrate that the loss of HJV membrane export is central to the pathogenesis of JH, and that HJV cleavage is essential for the export. The results support a dual function for s- and m-HJV in iron deficiency and overload, respectively. (Blood. 2007;109:4503-4510)

Introduction

The study of hereditary hemochromatosis (HH) has contributed major advances to our understanding of the systemic iron regulation.[1] The key regulatory protein is hepcidin, a small antimicrobial liver peptide[2] that has an inhibitory effect on the release of iron from duodenal cells and macrophages to the circulating transferrin.[3] Mutations of hepcidin cause a recessive form of severe, early-onset hemochromatosis, known as juvenile hemochromatosis (JH; type 2B HH).[4] The same severe phenotype is more commonly caused by mutations of *HJV*, the gene encoding hemojuvelin (type 2A HH).[3] Studies in humans and mice provide evidence that HJV positively modulates hepcidin expression. Urinary hepcidin levels are remarkably low in patients carrying *HJV* mutations,[5] and *Hjv*-deficient mice have dramatically decreased liver hepcidin mRNA.[6,7] The mechanism of hepcidin activation by HJV remains to be clarified. Recently, it has been shown that HJV could act as a bone morphogenetic protein (BMP) coreceptor, enhancing BMP-mediated signaling[8] and likely up-regulating hepcidin expression through BMP-activated SMA and MAD proteins (SMAD).[9]

HJV is highly homologous to proteins belonging to the family of repulsive guidance molecules (RGMs). In the mouse, the expression of Rgma and Rgmb is limited to developing and adult central nervous system, while Rgmc, the ortholog of human HJV, is detected in the same tissues (skeletal muscle, heart, and liver) where hepcidin is expressed.[3] Similar to RGM members, the *HJV* gene encodes a protein characterized by multiple domains, including a N-terminal signal peptide, a RGD integrin-binding motif, a partial von Willebrand factor (VWF) type D domain, and a C-terminal glycosilphosphatidylinositol (GPI) anchor domain. All RGM proteins possess a Gly-Asp-Pro-His (GDPH) sequence,[10,11] which undergoes a partial autocatalytic cleavage at the Asp-Pro bond at acidic pH, compatible with that of the late secretory pathway.[12] HJV is retained on the outer layer of the plasma membrane (m-HJV) through the GPI anchor motif, but can also be found as a soluble form (s-HJV) both in vitro and in vivo.[13,14]

Recent studies in murine muscle cells and fibroblasts have analyzed the complex biosynthesis of Rgmc during myoblast differentiation. Two classes of GPI anchor Rgmc molecules exist that are differently processed and have distinct fates: a membrane-associated heterodimer, composed of cleaved N- and C-terminal fragments, and a full-length form, prevalent in the extracellular fluid.[14]

About 30 distinct missense or nonsense point mutations have been identified in the *HJV* gene leading to JH.[3,15,16] In order to gain insights into the pathogenesis of this disorder and to characterize the functional properties of human HJV, we have studied the biosynthesis and maturation of 5 missense (G99V,[3] C119F,[16] F170S,[17] W191C,[17] and G320V[3]) and 1 nonsense (R326X[3]) allelic variants associated with JH. We demonstrate that mutants with defective autoproteolytic processing (F170S, W191C, and G320V) are not correctly targeted to the plasma membrane (PM) but are mainly retained in the endoplasmic reticulum (ER), as observed for the truncated R326X variant. We also find that in our model, the HJV mutants' ability to be released in the culture medium is independent from the membrane export. Finally, we show that iron negatively modulates the release of both wild-type (WT) and mutant s-HJV, while it has differential effects on m-HJV.

Submitted August 10, 2006; accepted January 23, 2007. Prepublished online as *Blood* First Edition Paper, January 30, 2007; DOI 10.1182/blood-2006-08-041004.

The online version of this article contains a data supplement.

The publication costs of this article were defrayed in part by page charge payment. Therefore, and solely to indicate this fact, this article is hereby marked "advertisement" in accordance with 18 USC section 1734.

Materials and methods

Generation of WT and HJV mutants

The whole *HJV* open-reading frame was amplified from human cDNA by using primers and cloning strategies described in Document S1, available on the *Blood* website (see the Supplemental Material link at the top of the online article). Mutant constructs were generated by site-directed mutagenesis by using oligonucleotides shown in Table S1.

Generation of anti-HJV

The DNA fragment encoding from amino acid 226 to 402 of human HJV was cloned into a pGEX (Amersham Biosciences Europe GmbH, Freiburg, Germany) vector in fusion with GST. The peptide comprises the C-terminal 176 amino acids of the protein deleted of the GPI anchor motif. The proteins were expressed in *Escherichia coli*, purified by affinity chromatography, and used to elicit antibodies in mice.

Cell culture

Cell culture media and reagents were from Invitrogen (Carlsbad, CA) and from Sigma-Aldrich (St Louis, MO). HeLa and HepG2 cells were cultured in Dulbecco modified Eagle medium (DMEM) supplemented with 2 mM L-glutamine, 200 U/mL penicillin, 200 mg/mL streptomycin, 1 mM sodium pyruvate, and 10% heat-inactivated fetal bovine serum (FBS) at 37°C in 95% humidifier air and 5% CO_2.

Western blot analysis

HeLa cells were seeded in 100-mm diameter dishes until 70% to 80% of confluence was reached. Cells were transfected with a complex consisting of 10 μg plasmid DNA and 30 μL of the liposomal transfection reagent Metafectene (Biontex Laboratories, Munich, Germany) in 4 mL OptiMem (Invitrogen) according to the manufacturer's instructions. HepG2 cells were transfected with 24 μg plasmid DNA and 60 μL Lipofectamine 2000 (Invitrogen), according to the manufacturer's instruction. After 18 hours the medium was replaced; cells were collected after 24 hours and lysed in RIPA buffer for Western blot analysis.

Proteins were quantified by using the Bio-Rad Protein Assay (Bio-Rad, Hercules, CA); samples (50 μg) were subjected to 10% or 15% SDS-PAGE, and were transferred to Hybond C membrane (Amersham Biosciences Europe) by standard Western blotting technique. Blots were incubated with the relevant primary antisera at dilutions recommended by the manufacturer. Anti-HJV was used at a proportion of 1:500. After washing in TBS (0.5 M Tris-HCl [pH 7.4] and 0.15 M NaCl) containing 0.1% Tween-20, blots were incubated with relevant HRP-conjugated secondary antisera and developed using a chemiluminescence detection kit (ECL; Amersham Biosciences Europe).

WT and R326X HJV precursor proteins were synthesized by in vitro transcription and translation (TNT-coupled reticulocyte lysate system; Promega, Madison, WI) following the manufacturer's instructions, resuspended in Laemmli sample buffer, and loaded on a 10% SDS-PAGE without boiling.

Endo H and PNGase F digestion

Endoglycosidase H (Endo H) and peptide N-glycosidase F (PNGase F) treatments essentially followed the manufacturer's (New England Biolabs, Ipswich, MA) protocols. Protein extracts were denatured in 0.5% SDS plus 1% β-mercaptoethanol at 100°C for 5 minutes, and incubated at 37°C with Endo H or PNGase F in the presence of the appropriate buffers. The reactions were stopped by adding Laemmli sample buffer and proteins analyzed by SDS-PAGE.

Analysis of s-HJV

HeLa cells were transiently transfected as described in "Western blot analysis," and media were replaced after 18 hours. Cells were incubated with serum-free media, which were collected after 24 hours, concentrated using 5-kDa molecular weight (MW) cut-off ultrafiltration (Amicon Ultra; Millipore, Billerica, MA) and analyzed by SDS-PAGE. When indicated, brefeldin A (BFA) was added to the serum-free media, and cells were incubated for 24 hours. Densitometric analysis was performed on 5 independent experiments using the ImageJ algorithm (http://rsb.info.nih.gov). The student *t* test was used for statistical calculations.

Cell-surface HJV expression

Quantitation by binding assay. A total of 10^4 HeLa cells were seeded in 48-well plates and transfected with 0.25 μg of plasmid DNA using 1 μL of the liposomal transfection reagent Metafectene according to the manufacturer's instructions. For HepG2 cell analysis, 0.4 μg of plasmid DNA were complexed with 1 μL Lipofectamine 2000. After 12 hours, the medium was replaced, and 24 hours later, cells were fixed with 4% paraformaldehyde for 30 minutes at room temperature. Cells were washed with PBS, blocked with 5% nonfat milk in PBS, incubated with anti-cMYC (1:250), and then with the relative secondary HRP antibody at 37°C. For total HJV expression, cells were permeabilized with 0.1% Triton X-100 in PBS, prior to blocking and incubation with anti-cMYC. Peroxidase activity was measured with an HSR substrate (o-phenylenediamine dihydrochloride; Sigma-Aldrich) according to the manufacturer's instructions. The amount of m-HJV was calculated as a ratio between the absorbance of unpermeabilized and permeabilized cells.[18] Background absorbance was subtracted for each sample. The Student *t* test was used for statistical calculation.

PI-PLC cleavage of membrane-bound HJV. A total of 10^6 HeLa cells, transiently transfected with HJV-expressing constructs or empty vector, were incubated in PBS or DMEM plus 0.3 U/mL phosphatidylinositol-specific phospholipase C (PI-PLC) at 37°C in a 5% CO_2 incubator. After 2 hours, the supernatants were collected, and proteins were precipitated with TCA or cold acetone and loaded on a 10% SDS-PAGE.

EM analyses

HeLa cells were transiently transfected with Lipofectamine using pcDNA3.1 expressing WT and mutant HJV. After transfection (18 hours), cells were fixed, labeled with a polyclonal goat anti-cMYC using the gold-enhance protocol, embedded in Epon-812, and cut as described previously.[19] Immunoelectron microscopy (EM) images were acquired from thin sections under a Philips Tecnai-12 electron microscope (Philips, Einhoven, the Netherlands) using an ULTRA VIEW CCD digital camera. Thin sections were also used to quantify gold particles residing within different compartments of the secretory pathway.

Membrane release assay of HJV

s-HJV release assay was performed essentially as described for the transferrin receptor.[20] After 36 hours from transfection, HeLa cells were washed with PBS (without calcium and magnesium), detached from the dishes, centrifuged at 1000*g* for 5 minutes, and washed with PBS. All the following steps were carried out at 4°C. The pelleted cells were resuspended in 0.35 M sucrose plus 5 mM HEPES (pH 7.4), homogenized by douncing 40 times in a Dounce homogenizer (Kontes Glass, Vineland, NJ), and differentially centrifuged at 5000*g* for 20 minutes, followed by 42 000*g* for 1 hour. The membrane pellet was washed with 0.35 M sucrose plus 5 mM HEPES (pH 7.4) and again centrifuged at 13 000*g* for 20 minutes. Transfected HeLa membrane fractions were incubated in aliquots of 50 μL for 18 hours at 4°C and at 37°C to block and activate a proteolytic process, respectively. The samples were then centrifuged at 13 000*g* for 20 minutes at 4°C, the membrane pellets and supernatants were analyzed by 10% SDS-PAGE under reducing conditions, and HJV was detected by immunostaining with anti-HJV.

Results

Maturation and processing of WT and mutant HJV

To analyze the biogenesis of WT and mutant HJV, we cloned the full-length human *HJV* coding sequence in a mammalian expression vector (pcDNA3.1), incorporating the cMYC tag at the

N-terminus, immediately downstream of the signal peptide (Figure 1A). Next, we introduced some pathogenic mutations altering conserved residues: G99V modifies the RGD domain, C119F removes a Cys predicted to be involved in a disulphide bridge, F170S modifies a Phe next to the catalytic consensus sequence GDPH, W191C introduces an extra Cys in the partial VWF type D domain, G320V at the C-terminus is the most common mutation in patients,[3] and R326X removes the 100 C-terminal residues, including the GPI anchor moiety and a glycosylation site.

In addition, the recombinant C-terminal sequence of HJV, deleted of the GPI anchor motif, was expressed in *E coli* and purified by affinity chromatography, and then used to elicit antibodies that recognize the C-terminus of the protein (Figure 1A).

We first addressed the question whether the mutations affect the HJV posttranslational modifications. HJV contains 3 potential N-linked glycosylation sites and is predicted to be a GPI anchor protein based on a consensus sequence proximal to the transmembrane domain. Different levels of glycosylation of the transfectant HJV modify the protein electrophoretic mobility. The in vitro–transcribed HJV migrates in SDS-PAGE with the expected MW of 46 kDa, whereas cell-associated HJV migrates with an apparent MW of approximately 50 kDa (Figure 1B), suggesting the addition of carbohydrate moieties. G99V, C119F, F170S, W191C, and G320V migrate, as does the WT protein, around 50 kDa (Figure S1A). The R326X mutation, lacking the last 100 amino acids and missing 2 C-terminal cysteines, migrates slower than the in vitro–synthesized corresponding mutant (Figure S1B; bottom panel).

To analyze in detail the glycosylation status of the mutants, the cellular extracts were digested with either Endo H or PNGase F and analyzed by Western blot. Endo H is specific for the Asn-linked high-mannose oligosaccharides produced in the early ER, while PNGase F also deglycosylates fully mature proteins, with complex oligosaccharides modified in the *trans* face of the Golgi apparatus. We find that Endo H converts the expressed WT and mutants to partially deglycosylated forms (Figure 1C); however, the pattern of F170S, W191C, and G320V is different from that of WT, suggesting they have an altered glycosylation process. After PNGase F treatment, the mobility of missense HJV mutants was analogous to that of the WT protein (Figure 1D). Moreover, Endo H and PNGase F modify R326X mobility to a similar extent, suggesting that this is not complex-glycosylated as the WT HJV (Figure 1E).

Mature HJV contains 14 cysteine residues, some of which are probably involved in intra- or interchain disulfide bonds and modify electrophoretic mobility. Thus, HeLa cells homogenates were analyzed in SDS-PAGE. Under reducing conditions, HJV migrates at approximately 50 kDa, while under nonreducing conditions, it migrates faster, at about 46 kDa, indicating a more compact conformation, likely caused by intramolecular disulfide bridges (Figure S1B). All missense mutations and R326X behave as the WT HJV, except C119F, which shows a broader band under nonreducing conditions.

HJV undergoes an autoproteolytic cleavage

RGMs are subjected to a proteolytic processing, through the cleavage at the GDPH consensus sequence,[12] similarly to other proteins, as mucin and BMPER.[21,22] Consistently, under reducing conditions, HJV shows a smaller band of approximately 33 kDa, in addition to the major approximately 50-kDa species (Figure 1B). The 33-kDa band is not detectable with anti-cMYC antibody, nor it visible under nonreducing conditions (data not shown), suggesting that it consists in a C-terminal fragment held to the cleaved product by disulfide bonds. The low amount of the expected 16-kDa N-terminal fragment, generated by the cleavage,[12,14] was not detectable, perhaps for the low sensitivity in blotting of the anti-cMYC antibody.

To understand whether the mutations alter the proteolytic processing, total lysates from transfected HeLa cells were analyzed under reducing conditions. As shown in Figure 2A, only G99V and C119F produce the 33-kDa fragment, while in F170S, W191C, and G320V variants, only the full-length, 50-kDa form is present. Similar results were obtained in HepG2 cells (Figure S2).

HJV mutants are highly reduced at the plasma membrane

We used a surface-labeling method[18] to investigate the amount of WT and HJV mutants localized on HeLa and HepG2 cell surfaces 36 hours after transfection. Plasma membrane (PM) of HeLa cells exposes almost identical amounts of WT and G99V HJV

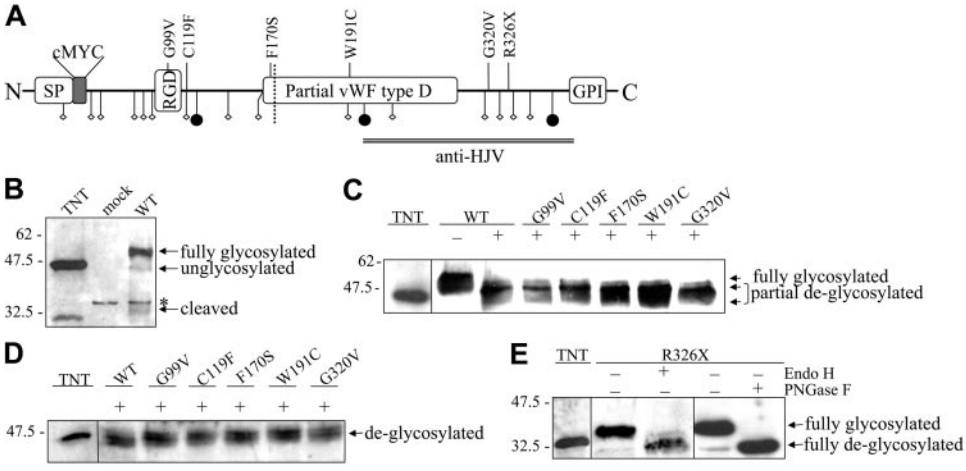

Figure 1. Maturation and processing of HJV. (A) Schematic representation of HJV functional domains and localization of the studied mutations. SP indicates signal peptide; RGD, arginine-glycine–aspartic acid integrin-binding domain; ◇, Cys residue; and ●, Asn residue. The dotted line indicates the autoproteolytic site. The double line shows the peptide chosen for antibody production. (B) Characterization of the mouse polyclonal anti-HJV. Hela cells were transfected with empty vector (mock) or WT HJV-expressing construct (WT). HJV was synthesized by in vitro transcription and translation (TNT). *Unspecific band. Anti-HJV recognizes a major band, which corresponds to the mature HJV, and a faint band derived from the autoproteolysis of the VWF type D domain. (C-D) WT and mutants HJV (30 μg of total lysates) were treated (+) with Endo H (C) or PNGase F (D) following manufacturer's instructions. (E) The nonsense R326X mutation produces a truncated HJV that is partially glycosylated, as shown by the band shift after Endo H and PNGase F treatment. The arrows show the glycosylation state. Scales refer to relative molecular mass in kilodaltons.

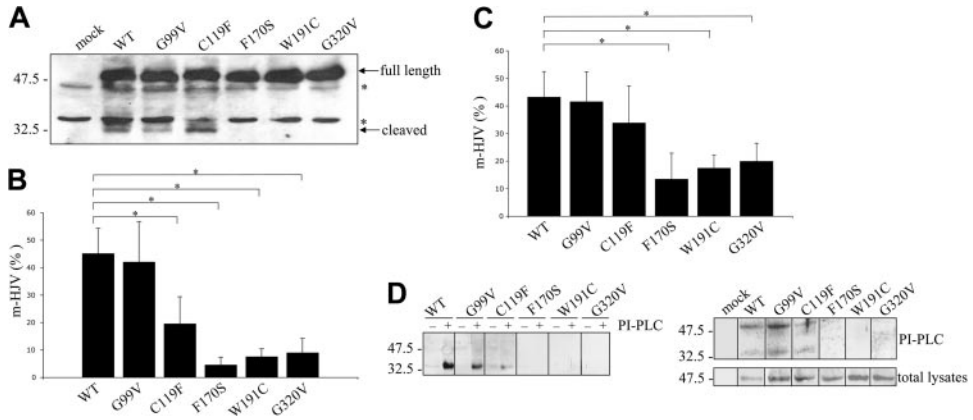

Figure 2. Analysis of the autoproteolytic cleavage and the cell-surface expression of HJV. (A) HeLa cells were transfected with empty vector (mock)–, WT-, and mutant HJV–expressing constructs; 50 μg of total lysates were loaded onto a 15% SDS-PAGE, blotted, and incubated with anti-HJV. Full-length (approximately 50 kDa) and cleaved (approximately 33 kDa) bands are indicated. *Unspecific bands. (B) Transfected HeLa cells were fixed and incubated with anti-cMYC. The amount of HJV expressed at the cell surface (nonpermeabilized cells) is shown as a fraction (percentage) of total protein expression (permeabilized cells). Statistical significance was calculated on 6 independent experiments, made in triplicate. *$P < .001$. (C) Transfected HepG2 cells were treated as described in panel A, and analyzed for the percentage of cell-surface HJV. *$P < .001$. (D) Top panel: transfected HeLa cells were incubated with (+) or without (−) PI-PLC (0.3 U/mL) in PBS at 37°C; after 2 hours, TCA-precipitated proteins were analyzed with anti-HJV. Bottom panel: transfected cells were incubated for 2 hours in DMEM containing 0.3 U/mL PI-PLC. Total lysates and acetone-precipitated proteins were analyzed under mildly reducing conditions with anti-HJV. Scales refer to relative molecular mass in kilodaltons. Error bars indicate SD.

(45.1% ± 9.2% and 42.0% ± 14.8%, respectively; Figure 2B). Also, the autoproteolytically active C119F variant reaches the PM, but less efficiently than WT (19.5% ± 9.9%). In contrast, m-HJV is reduced in the other mutants (F170S, 4.5% ± 2.9%; W191C, 7.5% ± 2.9%; and G320V, 8.9% ± 5.3%), indicating an impairment of the proper HJV trafficking and sorting to the cell surface (Figure 2B). The same assay in HepG2 cells confirmed an m-HJV reduction of F170S, W191C, and G320V, whereas C119F is more competent to localize to the cell surface (Figure 2C). Similar results were obtained by flow cytometry of nonpermeabilized HeLa and HepG2 cells (Figure S3A-B). These data confirm that only the mutants that undergo autoproteolytic processing have the ability to reach the PM.

To further analyze the characteristics of m-HJV, transfected HeLa cells were treated with PI-PLC, and the supernatant was analyzed. Analysis of the supernatants under reducing conditions show that WT, G99V, and C119F releases mainly the approximately 33-kDa form (Figure 2D; top panel). However, when the supernatants are analyzed under mildly reducing conditions, an additional slow-mobility band is detectable (Figure 2D; bottom panel), suggesting the existence of disulfide bonds that join the approximately 33-kDa and the approximately 16-kDa fragments together, as already described.[12-14] After PI-PLC treatments and under reducing conditions, trace amounts of the full-length approximately 50-kDa HJV is revealed by anti-cMYC, using only a highly sensitive detection method (ECL Advance; Amersham Biosciences Europe) confirming the low quantity of the uncleaved protein on the PM of WT and mutant transfected cells (data not shown). Altogether, these results indicate that the major type of m-HJV is the heterodimeric form derived from the autoproteolytic cleavage.

HJV mutants are selectively retained into the endoplasmic reticulum

To study the HJV mutants unable to reach the PM, EM and morphometric analysis on HeLa cells were performed 18 hours after transfection. As shown in Figure 3A and 3B, WT HJV is localized mainly on the PM, in part to the Golgi (G) and in low proportion into the endoplasmic reticulum (ER), suggesting a proper maturation pathway. On the contrary, C119F, W191C,

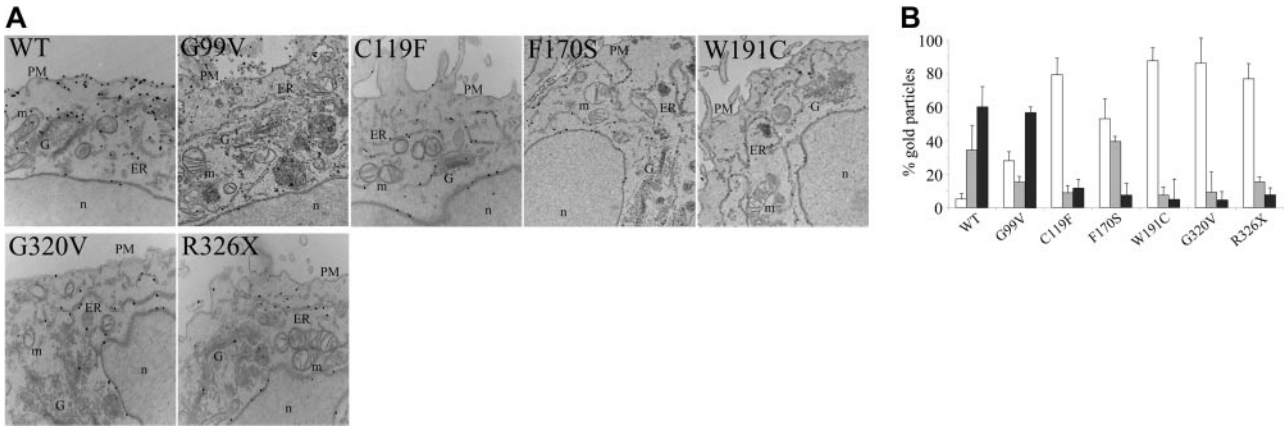

Figure 3. HJV mutants are retained into the ER. (A) HeLa cells were transiently transfected with mammalian vectors encoding WT and mutants HJV. At 18 hours after transfection, sections were stained with antibody against cMYC using nano-gold protocol as described in "Materials and methods." Images were acquired using AnalySIS software (Soft Imaging System, Lakewood, CO). Original magnification, × 23 000. PM indicates plasma membrane; ER, endoplasmic reticulum; G, Golgi; m, mitochondria; and n, nucleus. (B) Morphometric analysis of WT and mutant HJV proteins showing the different distribution of the molecule in intracellular compartments. □ indicates ER; ▨, Golgi apparatus; and ■, plasma membrane. Error bars indicate SD.

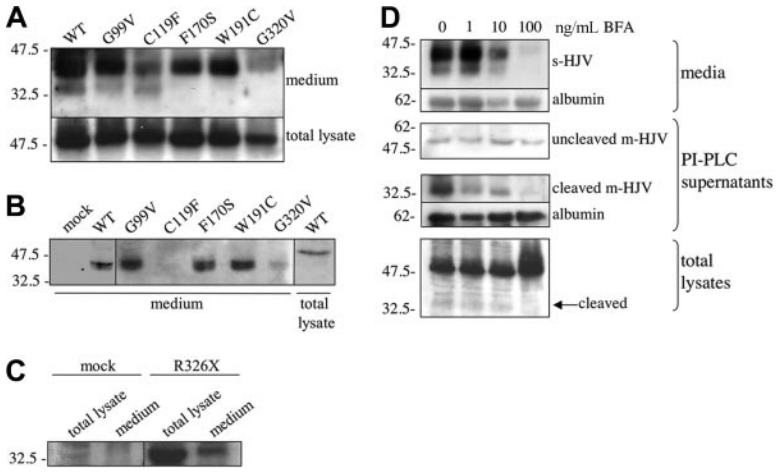

Figure 4. HJV is secreted in the medium through a BFA-dependent pathway. (A-B) Transfected HeLa cells were incubated for 24 hours in serum-free media. Total lysates (50 μg) and concentrated media were analyzed by using anti-HJV (A) and anti-cMYC (B). (C) R326X- or mock-transfected HeLa cells were incubated in DMEM with 2% FBS; after 2 hours, total lysates and TCA-precipitated media were analyzed by Western blot using anti-HJV. (D) BFA treatment of WT HJV-transfected HeLa cells. HeLa cells were incubated 24 hours with increasing amount of BFA. Concentrated media, PI-PLC supernatant, and total cellular lysates were loaded on 10% SDS-PAGE, and proteins were revealed by anti-HJV. The 50-kDa uncleaved m-HJV was detected by anti-cMYC. The relative molecular mass, in kilodaltons, is indicated on the left.

G320V, and R326X are predominantly clustered into the ER. The F170S cleavage variant shows labeling of Golgi and ER, and a minor one at PM, suggesting Golgi and ER retentions. A significant proportion of the G99V protein is found within the ER; nevertheless, this variant can still get to the cell surface quite efficiently in comparison with the others. Thus, the reduced expression on PM is probably due to the inappropriate protein folding or processing for all mutants, except G99V, where there may be a delay in the cell-surface localization.

HJV is released as a soluble form in the cell culture medium

To assess whether HJV is released in the medium, transiently transfected HeLa cells were grown in serum-free media for 24 hours at 37°C; then, cell culture supernatants were analyzed by using anti-HJV and anti-cMYC. Anti-HJV recognizes 2 different species: a major one of 42 kDa and a minor one of approximately 33 kDa detectable only in WT, G99V, and C119F (Figure 4A). The approximately 42-kDa species has faster mobility than the cell-associated HJV and is recognized also by the anti-cMYC (Figure 4B). Since cMYC is localized at the N-terminus of the protein, the truncation of s-HJV must take place at the C-terminus.

The total amount of soluble form is comparable in WT and mutants, except C119F and G320V, which are reduced (C119F, 62.4% ± 17.9%; G320V, 62.3% ± 27.7%; $P < .01$ vs WT). R326X, lacking the GPI anchor moiety, is efficiently secreted, and its soluble form has the same MW of the cellular form (Figure 4C).

BFA is a fungal antibiotic which efficiently inhibits protein maturation across the post-ER pathways.[23] To further study the posttranslational modification of HJV, WT-transfected HeLa cells were incubated with different concentrations of BFA and HJV analyzed in total lysates, PMs, and media (Figure 4D). After treatment with 100 ng/mL BFA, no band corresponding to s-HJV (42 and 33 kDa) is detectable in the medium, while the full-length cell-associated HJV is increased. In addition, the 33-kDa cleaved band is no more detectable in the cellular lysates, suggesting that at this concentration BFA blocks protein export from the *trans*-Golgi network (TGN; Figure 4D). These results suggest that both s-HJV and cleaved m-HJV follows a BFA-dependent maturation pathway.

Iron modulates the release of s-HJV

It has been previously demonstrated that the release of s-HJV is dependent upon iron quantity in the culture medium.[13] Under low-iron concentrations, HJV was efficiently released; when iron was added (both in the form of ferric ammonium citrate [FAC] or diferric transferrin), s-HJV progressively decreased.[13] In principle, iron could modulate HJV trafficking to the PM or influence cellular mechanisms releasing s-HJV. To address this question, transiently transfected HeLa cells were incubated for 24 hours in the presence or absence of 50 μM FAC, and the media were analyzed by Western blot.

As shown in Figure 5A, iron supplementation causes a decrease of s-HJV in WT and all mutants, indicating that the HJV variants are as iron sensitive as the WT. By using the surface-labeling method, a significant increase of m-HJV is evident after FAC incubation in WT, but not in the mutants (Figure 5B; data not shown). Thus, although the transfected cells regulate the release of the s-HJV variants in response to iron, they are unable to efficiently expose additional m-HJV molecules on the PM.

The protein released in the medium does not originate from m-HJV

The results of PI-PLC treatment indicate that the membrane exposes mainly the cleaved form of HJV. The larger size of s-HJV compared with m-HJV (42 kDa vs 33 kDa) and its efficient release even from the membrane-defective mutants suggest that in our system it does not originate from GPI shedding.

To demonstrate that s-HJV does not originate from a proteolytic cleavage of m-HJV, membranes isolated from transiently transfected HeLa cells were incubated at 4°C and at 37°C to block and activate a proteolytic process, respectively.[20] We found that isolated membranes are richer in the 33-kDa band than the total lysates

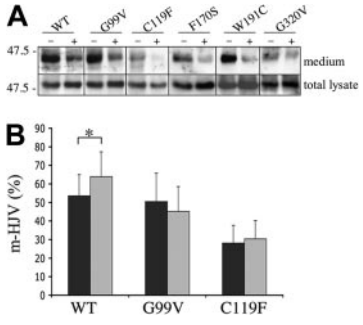

Figure 5. Iron modulates the secretion of s-HJV both in WT and mutants. (A) Transfected HeLa cells were incubated in serum-free media in the presence (+) or absence (−) of 50 μM FAC; after 24 hours, total lysates (50 μg) and concentrated media were analyzed with anti-HJV. Scales refer to relative molecular mass in kilodaltons. (B) Iron modulation of m-HJV was quantified by using the described binding assay. ■ indicates untreated cells; ▨, FAC-treated cells. Statistical significance was calculated on 4 independent experiments, made in triplicate. *$P < .05$. Error bars indicate SD.

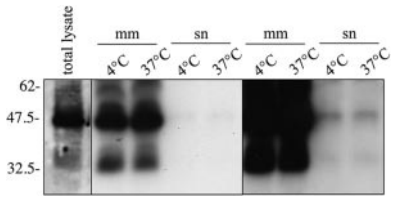

Figure 6. s-HJV does not originate from isolated membranes. Membrane fractions from WT HJV-transfected HeLa cells were incubated for 18 hours at 4°C and 37°C and centrifuged; the corresponding supernatants and membrane pellets were separated by 10% SDS-PAGE under reducing conditions. Right panel shows the same overexposed film. Proteins were revealed using anti-HJV. mm indicates microsomal membranes; sn, supernatant. The relative molecular mass, in kilodaltons, is indicated on the left.

(Figure 6), which is in agreement with m-HJV as a cleaved heterodimer. Trace amounts of 50-kDa and 33-kDa species in the supernatants were evident only when the film was overexposed and the band intensity after incubation at 4°C and 37°C was comparable. This suggests that the release of the 50-kDa and 33-kDa forms is unrelated to a proteolytic cleavage, but is likely unspecific and due to the large amount of cellular HJV in isolated membranes. We conclude that in our model the s-HJV is secreted.

Discussion

HJV mutations associated with JH are heterogeneous and widely spread along the gene-coding sequence. Although the evidence is that HJV up-regulates hepcidin, it is still unclear how mutations impair hepcidin activation, thereby causing the inappropriately high iron absorption and the severe iron loading that characterize the disease. Available studies concern the most frequent G320V mutation and the corresponding G313V of Rgmc, the murine ortholog of HJV. Human G320V was shown to be unable to interact with its putative receptor, neogenin, in HEK293 kidney cells,[12] while murine G313V caused a reduced enhancement of the endogenous BMP signaling that up-regulates hepcidin.[8] A similar defect was reported for the G99V human mutant.[8] Still, the reason for the failure of hepcidin activation remains unexplained.

To explore the biosynthesis and maturation of HJV mutants we developed an expression vector encoding 5 missense (G99V, C119F, F170S, W191C, and G320V) and 1 truncated (R326X) variants identified in patients. The analyses of transfected HeLa and HepG2 cells, expressing WT and mutant HJV, provide new information both on the processing of HJV to the membrane and cell medium, and on the impairments caused by the mutations.

Western blotting and Endo H and PGNase F digestions confirm that HJV has complex glycosylation moieties, indicating that it transits through the ER and Golgi apparatus. Like mucin and BMPER, which undergo an autocatalytic cleavage at the GDPH consensus sequence of the VWF domain,[21,22] HJV is also cleaved, giving rise to 2 fragments of approximately 33 and 16 kDa. In the transfected cells, WT HJV is present in the lysate as full-length (50 kDa) and cleaved (33 kDa) bands, at the cell surface mainly as the cleaved heterodimer, and in culture media mainly as an 42-kDa species, the cleaved form being a minor component. The cleaved species represents the major m-HJV form, as confirmed by the PI-PLC treatment, whereas a low amount of uncleaved 50-kDa m-HJV could be an artifact due to the overexpression of the exogenous protein. The 33-kDa form is undetectable in cellular lysates when BFA is added to cell culture at concentration that induces ER-Golgi fusion and blocks protein export from the TGN,[23] suggesting that the autocatalytic cleavage occurs in the late secretory pathway.[12]

R326X, which lacks the GPI anchor motif, is not present on the cell surface of the transfected HeLa and HepG2 cells, and the amount of membrane-associated isoforms is strongly reduced in both cell lines transfected with F170S, W191C, and G320V. Interestingly, the 33-kDa species is not observed in lysates of these transfectants (F170S, W191C, and G320V). In F170S it is likely that the Phe → Ser substitution at a residue adjacent to the GDPH sequence causes the inhibition of the autoproteolytic process. Defective cleavage is also observed in W191C and G320V. An abnormal protein conformation may be expected in W191C that introduces an extra, odd Cys, and possibly in G320V, where a more rigid Val substitutes a flexible and likely exposed Gly. That altered conformations can inhibit GDPH cleavage has already been demonstrated in pre–alpha-inhibitor heavy-chain precursor (pro-H3).[24] Thus, from the studies of W191C and G320V mutants, HJV cleavage seems to be related to proper folding, and consequently to proper maturation in ER/Golgi and export to the cell surface. This is supported by EM and morphometric analysis demonstrating that these 2 variants are mostly retained into the ER and less present into the Golgi, suggesting an ER retention mechanism, probably activated by the incorrect folding of the variants. Interestingly, F170S traffics more efficiently to the Golgi, indicating that this uncleaved mutant partially escapes from the ER control, perhaps because properly folded, but is still unable to reach the PM. This result suggests that autoproteolytic cleavage is necessary for export to the membrane and is compatible with it occurring beyond the ER, in the late secretory pathway. In agreement with this model, the G99V and C119F mutants, which are cleaved, find their way to the PM, although with different efficiency. We observed some differences in the amount of m-HJV according to the cell type used. In particular, the export of C119F is more efficient in HepG2 than in HeLa cells.

EM and morphometric analysis at 18 hours post-transfection show that G99V and C119F variants are also partially retained into the ER, while at 36 hours they are efficiently exposed on membranes, suggesting a delay in the cell-surface localization.

Altogether, our results indicate that altered maturation and reduced membrane localization characterize most of the mutants studied (Table 1), and likely are common mechanisms leading to HJV-associated JH. Other truncated variants (Q312X,[25] C321X,[26] and R385X[17]) probably share the same pathogenetic mechanism with R326X, and the cleavage is expected to be inhibited in A168D[15] and D172E,[15] which occur close to and within the GDPH motif, respectively. Reduction of m-HJV impairs the activation of the signal pathway involved in hepcidin up-regulation.[9] The pathogenetic mechanism of G99V and C119F that are present on the PM, although show some maturation defects, remains to be fully elucidated. We hypothesize a defect of the binding to the ligand (BMP) or to coreceptors, which

Table 1. Scheme of maturation and processing of the WT and mutant HJV

	WT	G99V	C119F	F170S	W191C	G320V	R326X
ER	+	++	+++	+++	+++	+++	+++
Golgi	+++	++	+	+++	+	+	+
GDPH cleavage	Yes	Yes	Yes	No	No	No	ND
PM	+++	+++	++	+	+	+	–
Medium	+++	+++	+	+++	+++	+	+++

ND indicates not determined.

generates the inadequate activation signal for hepcidin production, as demonstrated for G99V.[8]

Cleavage of the GPI anchor protein by membrane-associated phospholipases or proteases represents a common mechanism to release the soluble counterparts of GPI-anchored proteins in extracellular fluid.[27] However, the activity of phospholipases and proteases would not be selective in discriminating the different GPI-anchored proteins, suggesting the possibility of alternative mechanisms.[28] HeLa cells release s-HJV into the medium mainly as an approximately 42-kDa species, as HEK293 and Hep3B cells do.[13] This species is efficiently released from all mutants, with the exception of C119F and G320V, and without any relationship with the amount of m-HJV. A faint band of released 33 kDa is detected only in WT and some variants. That the soluble 42-kDa form cannot be derived from a protease-mediated shedding of m-HJV is supported by the following findings: (1) the discrepancy between the amount of membrane and soluble forms observed in some variants; (2) the evidence that PI-PLC releases mainly the 33-kDa cleaved moiety from the membrane; and (3) the absence of the 42-kDa isoform in isolated membrane supernatant. Thus, the 42-kDa s-HJV seems to derive from an independent secretory pathway, as reported for the GPI anchor folic acid receptor.[28] The minor band of 33 kDa found in the soluble fractions of the variants competent for the cleavage process could represent their soluble autocatalytic product, as reported for MUC5AC.[29] Whether this secretory mechanism is the result of HJV overexpression, or whether it occurs in physiologic conditions and in which cell types, remains to be established.

A partial processing of mouse G313V Rgmc has been recently described. Lack of cleavage was shown in transfected Cos-7 cells, although in that system some uncleaved protein reaches the PM and may release some Rgmc.[14] We believe that the discrepancy with our results could be due to the high level of overexpression of the murine variant, caused by adenovirus infection, or to a different maturation process of the variant in nonmurine cells.

To understand whether both m- and s-HJV are involved in the pathogenesis of JH, we studied the effect of iron addition to the transfected cells. As previously shown for WT,[13] iron addition reduces the release into the medium of both WT and mutant s-HJV. On the contrary, WT, but none of the mutants present on the cell surface, responds to iron treatment by increasing m-HJV. These findings strengthen the central role of m-HJV in the disease. s-HJV might fulfill the function of sequestering BMP to inhibit both BMP signaling and hepcidin expression,[8] which is compatible with a role in signaling iron deficiency.[13] The finding that s-HJV is strongly reduced by iron in all mutants as well as in WT is in agreement with this interpretation and indicates that s-HJV has a minor role, if any, in the disease.

Our results are consistent with the proposed dual role of HJV in iron metabolism: s- and m-HJV might reciprocally regulate hepcidin expression in response to iron changes,[13] and depending on the different cell types. m-HJV could be most important in the hepatocytes, where the protein behaves as BMP coreceptor to respond to iron excess up-regulating hepcidin. In other cells, which do not express hepcidin, such as skeletal muscle cells,[14] the significance of m-HJV remains unclear, while s-HJV secretion could signal the iron needs.[13] Whether s-HJV binds BMP and/or antagonizes its effect on membrane receptors remains to be established.

Acknowledgments

We thank Roman Polishchuk from the Telethon Electron Microscopy Core Facility (TeEMCoF; Consorzio Mario Negri Sud–Santa Maria Imbaro) for the immuno-EM and morphometric analysis on HJV proteins. We thank also Giorgio Biasiotto and Maura Poli for the production and characterization of recombinant HJV fragment and anti-HJV antibodies.

Supported by the Italian Telethon Foundation ONLUS Rome Grant GGP05024 to C.C., grants from Ministero Istruzione, Università e Ricerca, Rome, Italy (PRIN 2004) to C.C. and P.A., and EU contract no. LSHM-CT-2006-037296 to C.C. and P.A.

Authorship

Author contributions: L.S. designed the experimental work, performed research, and wrote the manuscript; A.P. performed research and analyzed data; C.F. and G.G. performed research; S.L. helped design research and analyze data; P.A. contributed to analyze data and to write the manuscript; and C.C. designed research and wrote the manuscript.

Conflict-of-interest statement: The authors declare no competing financial interests.

Correspondence: Clara Camaschella, Università Vita-Salute San Raffaele, Via Olgettina, 60, 20132 Milano, Italy; e-mail: clara.camaschella@hsr.it.

References

1. Camaschella C. Understanding iron homeostasis through genetic analysis of hemochromatosis and related disorders. Blood. 2005;106:3710-3717.
2. Nemeth E, Ganz T. Regulation of iron metabolism by hepcidin. Annu Rev Nutr. 2006;26:323-342.
3. Papanikolaou G, Samuels ME, Ludwig EH, et al. Mutations in HFE2 cause iron overload in chromosome 1q-linked juvenile hemochromatosis. Nat Genet. 2004;36:77-82.
4. Roetto A, Papanikolaou G, Politou M, et al. Mutant antimicrobial peptide hepcidin is associated with severe juvenile hemochromatosis. Nat Genet. 2003;33:21-22.
5. Papanikolaou G, Tzilianos M, Christakis JI, et al. Hepcidin in iron overload disorders. Blood. 2005; 105:4103-4105.
6. Niederkofler V, Salie R, Arber S. Hemojuvelin is essential for dietary iron sensing, and its mutation leads to severe iron overload. J Clin Invest. 2005; 115:2180-2186.
7. Huang FW, Pinkus JL, Pinkus GS, Fleming MD, Andrews NC. A mouse model of juvenile hemochromatosis. J Clin Invest. 2005;115:2187-2191.
8. Babitt JL, Huang FW, Wrighting DM, et al. Bone morphogenetic protein signaling by hemojuvelin regulates hepcidin expression. Nat Genet. 2006; 38:531-539.
9. Wang RH, Li C, Xu X, et al. A role of SMAD4 in iron metabolism through the positive regulation of hepcidin expression. Cell Metab. 2005;2:399-409.
10. Monnier PP, Sierra A, Macchi P, et al. RGM is a repulsive guidance molecule for retinal axons. Nature. 2002;419:392-395.
11. Schmidtmer J, Engelkamp D. Isolation and expression pattern of three mouse homologues of chick Rgm. Gene Expr Patterns. 2004;4:105-110.
12. Zhang AS, West AP Jr, Wyman AE, Bjorkman PJ, Enns CA. Interaction of hemojuvelin with neogenin results in iron accumulation in human embryonic kidney 293 cells. J Biol Chem. 2005;280: 33885-33894.
13. Lin L, Goldberg YP, Ganz T. Competitive regulation of hepcidin mRNA by soluble and cell-associated hemojuvelin. Blood. 2005;106:2884-2889.
14. Kuninger D, Kuns-Hashimoto R, Kuzmickas R, Rotwein P. Complex biosynthesis of the muscle-enriched iron regulator RGMc. J Cell Sci. 2006; 119:3273-3283.
15. Lanzara C, Roetto A, Daraio F, et al. Spectrum of hemojuvelin gene mutations in 1q-linked juvenile hemochromatosis. Blood. 2004;103:4317-4321.
16. Gehrke SG, Pietrangelo A, Kascak M, et al. HJV gene mutations in European patients with juvenile hemochromatosis. Clin Genet. 2005;67:425-428.
17. De Gobbi M, Roetto A, Piperno A, et al. Natural history of juvenile haemochromatosis. Br J Haematol. 2002;117:973-979.

18. Lam-Yuk-Tseung S, Camaschella C, Iolascon A, Gros P. A novel R416C mutation in human DMT1 (SLC11A2) displays pleiotropic effects on function and causes microcytic anemia and hepatic iron overload. Blood Cells Mol Dis. 2006;36:347-354.
19. Polishchuk EV, Di Pentima A, Luini A, Polishchuk RS. Mechanism of constitutive export from the golgi: bulk flow via the formation, protrusion, and en bloc cleavage of large trans-golgi network tubular domains. Mol Biol Cell. 2003;14:4470-4485.
20. Kaup M, Dassler K, Weise C, Fuchs H. Shedding of the transferrin receptor is mediated constitutively by an integral membrane metalloprotease sensitive to tumor necrosis factor alpha protease inhibitor-2. J Biol Chem. 2002;277:38494-38502.
21. Lidell ME, Johansson ME, Hansson GC. An autocatalytic cleavage in the C terminus of the human MUC2 mucin occurs at the low pH of the late secretory pathway. J Biol Chem. 2003;278:13944-13951.
22. Moser M, Binder O, Wu Y, et al. BMPER, a novel endothelial cell precursor-derived protein, antagonizes bone morphogenetic protein signaling and endothelial cell differentiation. Mol Cell Biol. 2003;23:5664-5679.
23. Traub LM, Kornfeld S. The trans-Golgi network: a late secretory sorting station. Curr Opin Cell Biol. 1997;9:527-533.
24. Thuveson M, Fries E. The low pH in trans-Golgi triggers autocatalytic cleavage of pre-alpha -inhibitor heavy chain precursor. J Biol Chem. 2000; 275:30996-31000.
25. Koyama C, Hayashi H, Wakusawa S, et al. Three patients with middle-age-onset hemochromatosis caused by novel mutations in the hemojuvelin gene. J Hepatol. 2005;43:740-742.
26. Huang FW, Rubio-Aliaga I, Kushner JP, Andrews NC, Fleming MD. Identification of a novel mutation (C321X) in HJV. Blood. 2004;104:2176-2177.
27. Ferguson MA. Colworth Medal lecture: glycosylphosphatidylinositol membrane anchors: the tale of a tail. Biochem Soc Trans. 1992;20:243-256.
28. Wang J, Shen F, Yan W, Wu M, Ratnam M. Proteolysis of the carboxyl-terminal GPI signal independent of GPI modification as a mechanism for selective protein secretion. Biochemistry. 1997; 36:14583-14592.
29. Lidell ME, Hansson GC. Cleavage in the GDPH sequence of the C-terminal cysteine-rich part of the human MUC5AC mucin. Biochem J. 2006; 399:121-129.